

s*-Channel Dominance and Charge Ratios in High-Energy Pion Photoproduction

I. Barbour and W. Malone

Department of Natural Philosophy, Glasgow University, Glasgow, Scotland

and

R. G. Moorhouse†

Department of Physics and Lawrence Radiation Laboratory, University of California, Berkeley, California 94720

(Received 28 April 1971)

It is shown that an explicit quark model, or duality diagrams, imply certain charge ratios of the squares of the imaginary parts of the amplitudes for $\gamma N \rightarrow \pi^\pm N$ and $\gamma N \rightarrow \pi^\pm \Delta$, which are observed to hold in experiments on the high-energy cross sections $d\sigma/dt$ for $-0.2 \geq t \geq -0.8 \text{ GeV}^2$. A fixed- t dispersion-relation calculation, using knowledge of the low-energy photoproduction amplitudes, suggests that this may be due to cancellation of the contribution of the low- and medium-energy s - and u -channel resonances to the real parts of the amplitudes, so that the s channel dominates the dispersion integral, and the quark-model relations also apply to the real parts of the amplitudes. In the extreme forward direction [$(-t)^{1/2} \lesssim 0.2$] the fixed- t dispersion relations indicate that the $\gamma N \rightarrow \pi^\pm N$ amplitudes are predominantly real and dominated by the contributions to the dispersion relations of the Born approximation and other very-low-energy resonances. Some possible implications for purely hadronic reactions are discussed.

I. INTRODUCTION

It is well known that the differential cross section for $\gamma p \rightarrow \pi^+ n$ exhibits a forward spike in the region $0 > t \geq -m_\pi^2$ and that a similar forward spike is given by the gauge-invariant pion pole (electric Born approximation). Indeed, either the electric Born approximation or the full Born approximation¹ gives fair agreement with the data,² for both unpolarized and polarized photons³ in the spike region, except perhaps for the most forward points measured, as discussed below.

Likewise the differential cross section for $\gamma n \rightarrow \pi^- p$ for $0 > t \geq -m_\pi^2$ is found to be equal⁴ to that for π^+ photoproduction and thus also to be given approximately by the Born approximation. But for $-m_\pi^2 > t$ the Born approximation fails badly for both π^+ and π^- photoproduction; in particular, one of the most marked features of the data at high energy is that π^- photoproduction is less than π^+ photoproduction away from the forward-spike region. For $-0.2 > t > -0.8 \text{ GeV}^2$,

$$\frac{d\sigma}{dt}(\gamma n \rightarrow \pi^- p) / \frac{d\sigma}{dt}(\gamma p \rightarrow \pi^+ n) \approx 0.35. \quad (1)$$

Rather similar though more complicated features exist in the high-energy differential cross sections of the four reactions $\gamma N \rightarrow \pi^\pm \Delta$. It has been shown that for $0 > t > -m_\pi^2$, the differential cross sections are given, within their rather large errors, by a gauge-invariant pion-pole theory⁵ (in this case the minimal part of the Born approximation that both contains the pion pole and is gauge-invariant). For

$0 > t > -m_\pi^2$ the experiments are compatible with

$$\frac{d\sigma}{dt}(\gamma p \rightarrow \pi^- \Delta^{++}) = \frac{d\sigma}{dt}(\gamma n \rightarrow \pi^+ \Delta^-)$$

and

$$\frac{d\sigma}{dt}(\gamma p \rightarrow \pi^+ \Delta^0) = \frac{d\sigma}{dt}(\gamma n \rightarrow \pi^- \Delta^+),$$

in accord with a gauge-invariant pion-pole theory.⁵ However, away from the extreme forward direction these cross sections take on remarkably different ratios, as shown in Fig. 1. In the same region of t for which the ratio (1) holds, namely, $-0.2 > t > -0.8 \text{ GeV}^2$, the $\pi^\pm \Delta$ photoproduction cross sections take the following rather constant ratios:

$$\frac{d\sigma}{dt}(\gamma n \rightarrow \pi^- \Delta^+) / \frac{d\sigma}{dt}(\gamma p \rightarrow \pi^+ \Delta^0) \approx 0.3, \quad (2a)$$

$$\frac{d\sigma}{dt}(\gamma p \rightarrow \pi^- \Delta^{++}) / \frac{d\sigma}{dt}(\gamma n \rightarrow \pi^+ \Delta^-) \approx 0.5, \quad (2b)$$

$$\frac{d\sigma}{dt}(\gamma p \rightarrow \pi^- \Delta^{++}) / \frac{d\sigma}{dt}(\gamma p \rightarrow \pi^+ \Delta^0) \approx 1.0. \quad (2c)$$

It seems that the high-energy experiments on the forward photoproduction of charged pions exhibit three regions of t where the data have definite and distinct characteristics, though in all three regions $(s - M^2)^2 d\sigma/dt$ is approximately constant as a function of s .

(i) $0 > t > -m_\pi^2$. In this region the amplitudes are strongly affected by the exchange of the gauge-invariant pion pole (the energy dependence of this Born approximation agreeing with the observed en-

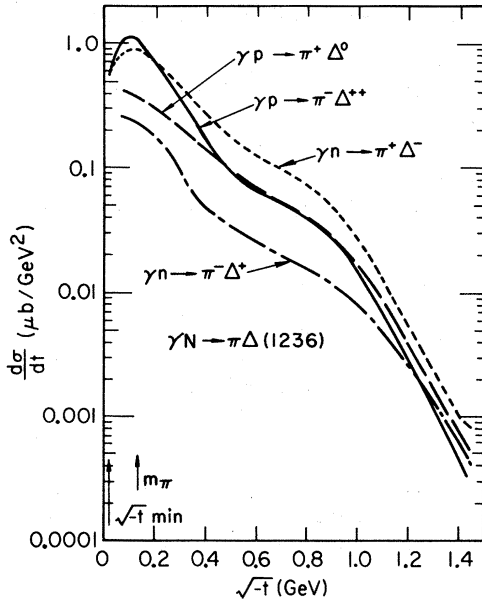


FIG. 1. High-energy differential cross sections for the processes $\gamma N \rightarrow \pi^\pm \Delta$.

ergy dependence). The π^+n and π^-p photoproduction cross sections are equal.

(ii) $-0.2 \geq t \geq -0.8 \text{ GeV}^2$. The charge ratios for π^+n and $\pi^+\Delta$ photoproduction are given by (1) and (2) throughout the region. In $\pi^+\Delta$ photoproduction the logarithmic slopes of $d\sigma/dt$ are constant to within the errors and approximately equal to $e^{2.5t}$; for π^+n the slope is approximately $e^{1.8t}$.⁴ Denote the cross sections corresponding to photons polarized perpendicular and parallel to the production plane by σ_\perp and σ_\parallel , respectively, then by Stichel's theorem σ_\perp and σ_\parallel correspond to natural- and unnatural-parity t -channel exchange, respectively. In $\gamma p \rightarrow \pi^+n$, σ_\perp is strongly dominant while in $\gamma n \rightarrow \pi^-p$, $\sigma_\perp = \sigma_\parallel$.

(iii) $-0.8 \text{ GeV}^2 > t > (?)$. In this region the charge ratios change and the slopes of the differential cross sections become steeper, the $\pi^+\Delta$ slope being about $e^{3.2t}$ and the π^+n slope about $e^{3.8t}$.⁴

It appears that the extreme forward region, (i) above, is partly understood in terms of the Born approximation or a similar theory, and we shall have some comment on that situation. It is the main object of this paper to contribute to the understanding of the region (ii), $-0.2 \geq t \geq -0.8 \text{ GeV}^2$, and in particular the charge ratios (1) and (2).

First, it is rather clear that no simple Regge-pole picture can satisfy the data in region (ii). The obviously dominant candidates for natural-parity exchange (measured by σ_\perp) are the exchange-degenerate ρ and A_2 trajectories contributing $\beta_\rho(t) \times (1 - e^{-i\pi\alpha(t)})/\sin\pi\alpha(t) + \beta_A(t)(1 + e^{-i\pi\alpha(t)})/\sin\pi\alpha(t)$ to the amplitudes, with $\alpha(t) = 0$ at $t \approx -0.6 \text{ GeV}^2$.

Strong exchange degeneracy with $\beta_A = \beta_\rho$ would give a dip in $\sigma_\perp(\gamma p \rightarrow \pi^+n)$ from the necessity that $\beta_A = 0$ at $t \approx 0.6 \text{ GeV}^2$; such a dip is conspicuously absent. Weak exchange degeneracy, $\beta_A \neq \beta_\rho$, could perhaps avoid the dip, but would lead to a purely real A_2 exchange amplitude (isovector photon) and a purely imaginary ρ exchange amplitude (isoscalar photon) at $t = -0.6 \text{ GeV}^2$. Since the difference between $\gamma p \rightarrow \pi^+n$ and $\gamma n \rightarrow \pi^-p$ photoproduction comes from the isoscalar-photon-isovector-photon interference term, this implies that $\sigma_\perp(\gamma p \rightarrow \pi^+n)$ would equal $\sigma_\perp(\gamma n \rightarrow \pi^-p)$ at $t \approx -0.6 \text{ GeV}^2$, contrary to the observed ratio of about 4 to 1. Thus it is evident that an explanation in terms of Regge theory requires cuts. For example, using the strong absorption model, and varying 28 parameters, Kane *et al.*⁶ obtain a fit to $\gamma p \rightarrow \pi^+n$, $\gamma n \rightarrow \pi^-p$ (and $\gamma p \rightarrow \pi^0p$, $\gamma p \rightarrow np$ and $\bar{p}p \rightarrow \bar{n}n$, $np \rightarrow pn$).

We attempt a unified view of the charge ratios (1) and (2a), (2b), (2c) first by considering the nucleon, and the Δ , as mainly composed of three quarks and by considering the process of photoproduction as one in which the nucleon is first photoexcited and then de-excited by pion emission. The basic quark diagram is shown in Fig. 2(a); the photon excites virtual intermediate states of the quark which decay by pion emission; if the quark is spatially excited, and does not de-excite by interaction with the other two quarks in the diagram, the sum over intermediate states points out the excited quark as the one which emits the pion leading to a quark impulse approximation.

In calculating the ratios (1), (2a), (2b), (2c) in the foregoing quark model, the spin and isospin sums over the intermediate quark states are replaced by the unit operator and, apart from the spatial factors, one is left with matrix elements of the form

$$\sum_{i=1}^3 \langle N | H^i(\gamma) H^i(\pi) | N \rangle, \quad \sum_{i=1}^3 \langle N | H^i(\gamma) H^i(\pi) | \Delta \rangle. \quad (3)$$

In (3) $|N\rangle$ and $|\Delta\rangle$ are $SU(6)$ wave functions of the $\{56\}$ representation for the nucleon and Δ , respectively; $H^i(\gamma)$ and $H^i(\pi)$ are the interaction Hamiltonians of the i th quark with the photon and pion, respectively. The isospin suboperator part of $H^i(\gamma)H^i(\pi)$ is, with the usual electromagnetic couplings of the quarks, proportional to

$$\begin{pmatrix} \frac{2}{3} & 0 \\ 0 & -\frac{1}{3} \end{pmatrix}_i \vec{\tau}^{(i)} \cdot \vec{\pi}. \quad (4)$$

In evaluating the ratios (1) and (2) in our model, the spin and spatial matrix elements cancel, whatever the particular form assumed for the interaction. The operator (4) gives rise to the following ratios:

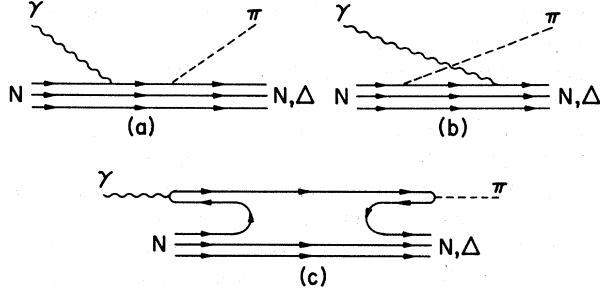


FIG. 2. (a) Quark-model diagram for pion photoproduction with s -channel excitation only. (b) Crossed diagram representing u -channel excitation only. (c) Duality diagram, equivalent to (a).

$$\frac{d\sigma}{dt}(\gamma n \rightarrow \pi^- p) \Big/ \frac{d\sigma}{dt}(\gamma p \rightarrow \pi^+ n) = \frac{1}{4}, \quad (5)$$

$$\frac{d\sigma}{dt}(\gamma n \rightarrow \pi^- \Delta^+) \Big/ \frac{d\sigma}{dt}(\gamma p \rightarrow \pi^+ \Delta^0) = \frac{1}{4}, \quad (6a)$$

$$\frac{d\sigma}{dt}(\gamma p \rightarrow \pi^- \Delta^{++}) \Big/ \frac{d\sigma}{dt}(\gamma n \rightarrow \pi^+ \Delta^-) = \frac{1}{4}, \quad (6b)$$

$$\frac{d\sigma}{dt}(\gamma p \rightarrow \pi^- \Delta^{++}) \Big/ \frac{d\sigma}{dt}(\gamma p \rightarrow \pi^+ \Delta^0) = \frac{3}{4}. \quad (6c)$$

The values (5), (6a), (6b) are, in the context of the model, an immediate consequence of the fact that a π^+ can only be emitted from a proton quark [involving the matrix element $\frac{2}{3}$ in (4)] and a π^- can only be emitted from a neutron quark [involving the factor $-\frac{1}{3}$ in (4)]. In the region $-0.2 \geq t \geq -0.8 \text{ GeV}^2$ the experimental values (1), (2a), (2b), (2c) are to be compared with (5), (6a), (6b), (6c), respectively. We note that there is almost quantitative agreement, and we notice (as displayed for example in Fig. 1) the remarkable change from the experimental ratios in the pion-pole region ($0 > t > -m_\pi^2$).

An important question in this picture is the possible contributions of the crossed graphs, Fig. 2(b), which have been ignored. It is immediately seen that these give contributions whose charge ratios are the inverses of (5), (6a), and (6b) so that a large contribution from the crossed graphs would invalidate our ratios. The uncrossed graphs [Fig. 2(a)] give the ratios corresponding to the contributions of s -channel resonances, and the crossed graphs [Fig. 2(b)] give the contributions of u -channel resonances. The u -channel resonances are distant from the forward direction so one expects their contributions to the imaginary part of the amplitudes to be small, but distant u -channel and distant s -channel resonances might dominate the real part. This is evidently happening for the particular case where the resonance is the nucleon itself at $t=0$ where the Born approximation is big and leads to

equal amplitudes for $\gamma p \rightarrow \pi^+ n$ and $\gamma n \rightarrow \pi^- p$, as observed.

One may put these questions in terms of the usual duality picture. If one assumes vector dominance, so that the isoscalar photon is represented by an ω meson and the isovector photon by a ρ^0 meson, then the selection rules implied by the duality diagrams will give relations between the *imaginary parts* of various photoproduction amplitudes.⁷ Among these relations for the imaginary parts are our ratios for $\gamma N \rightarrow \pi^\pm N$ and $\gamma N \rightarrow \pi^\pm \Delta$. [This is immediate on looking at Fig. 2(c), which pictures a photon turning into a vector meson, followed by a duality diagram for a vector meson scattering from a baryon into a pion. This figure is just a stretched-string version of Fig. 2(a), but not, of course, Fig. 2(b).] The figure also illustrates that in these relations the full vector-dominance assumptions are *not* being used, but only the relations between photon coupling to isoscalar and isovector mesons which follow from the photon being a U -spin scalar member of an octet. Such relations seem likely to endure strong modifications of the vector-dominance hypothesis, such as the addition of further

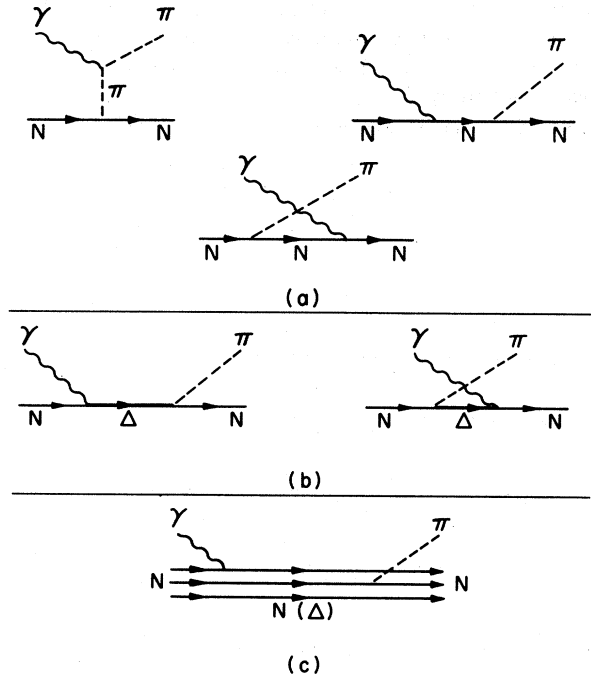


FIG. 3. (a) Feynman diagrams of Born-approximation amplitudes for $\gamma N \rightarrow \pi^\pm N$; these amplitudes give a forward spike in the cross section. (b) Quasi-Born-approximation amplitudes for $\gamma N \rightarrow \pi^\pm N$, with Δ instead of N as an intermediate state; these terms when combined with (a) give a more pronounced forward spike. (c) Schematic quark-model diagram contributing to the Born or quasi-Born amplitudes.

vector mesons through which the photon interacts with hadronic matter. These duality relations are *not* ensured for the real parts, just for the same reasons as mentioned above, namely, the possibility of large u -channel contributions to the real parts.

Nevertheless, the charge ratios indicate that the u -channel contributions are suppressed and we will seek verification and elucidation of this point by investigating, as explicitly as possible, the relative importance of the s - and u -channel contributions to the real part of the high-energy amplitude. The most direct way to do this is through fixed- t dispersion relations, and the results of such an investigation are reported in Sec. II.

II. s - AND u -CHANNEL CONTRIBUTIONS TO THE HIGH-ENERGY REAL PARTS OF AMPLITUDES

We wish to consider the relative contributions of the s and u channels to the real parts of the high-energy photoproduction amplitudes, and the most direct way of doing this is through the fixed- t dispersion relations. Because of the lack of detailed low-energy data on $\gamma N \rightarrow \pi^{\pm} \Delta$ we will have to confine most of the discussion in this section to $\gamma N \rightarrow \pi^{\pm} N$. For either of these processes there are four invariant amplitudes which we will denote by $A_{i+}(s, t)$ for $\gamma p \rightarrow \pi^+ n$ and by $A_{i-}(s, t)$ for $\gamma n \rightarrow \pi^- p$, where $i = 1, 2, 3, 4$. The fixed- t dispersion relations are³

$$\text{Re}A_{i\pm}(s, t) = B_{i\pm}(s, u) + \int_{(M+m)^2}^{\infty} ds' \left(\frac{\text{Im}A_{i\pm}(s', t)}{s' - s} + \xi_i \frac{\text{Im}A_{i\mp}(s', t)}{s' - u} \right), \quad (7a)$$

where the Born terms (see Fig. 3) are given by

$$\begin{aligned} B_{1+}(s, u) &= \sqrt{2} \frac{ge}{4\pi} \frac{1}{s - M^2}, \\ B_{2+}(s, u) &= -\sqrt{2} \frac{ge}{4\pi} \frac{1}{(s - M^2)(t - m^2)}, \\ B_{3+}(s, u) &= -\sqrt{2} \frac{ge}{4\pi} \frac{1}{2M} \left(\frac{\mu'_p}{s - M^2} - \frac{\mu'_n}{u - M^2} \right), \\ B_{4+}(s, u) &= -\sqrt{2} \frac{ge}{4\pi} \frac{1}{2M} \left(\frac{\mu'_p}{s - M^2} + \frac{\mu'_n}{u - M^2} \right), \\ B_{i-}(s, u) &= \xi_i B_{i+}(u, s). \end{aligned} \quad (7b)$$

In (7a) and (7b) $\xi_i = +1$ if $i = 1, 2, 4$ and $\xi_3 = -1$, M is the nucleon and m the pion mass. The first integral is over the s -channel cut and the second integral comes from the u -channel cut. The cut structure is shown in Fig. 4. In a quark, or duality-diagram, picture the amplitude ratios $\frac{1}{2}, \sqrt{\frac{3}{4}}$ lead-

ing to the ratios (5), (6a), (6b), and (6c) will hold between the appropriate $\text{Im}A(s', t)$ on the s -channel cut, as shown in Sec. I. However, the $\frac{1}{2}$ ratios will not hold for the $\text{Im}A$ on the u -channel cut, which corresponds to u -channel resonances, as in Fig. 2(b), rather than s -channel resonances, as in Fig. 2(a). For high-energy photoproduction, though the u -channel cut is distant from the physical s , we certainly cannot say *a priori* that the s -channel cut will dominate the right-hand side of Eq. (7). In pion photoproduction itself near $t=0$ we already know that the s - and u -channel Born poles, which are near together and both very distant from the physical s , are both very important in $\text{Re}A(s, t)$ implying an equal importance of an " s -cut" and a " u -cut" contribution. Near $t=0$, then, all is consistent with a totally real amplitude, into which the Born terms and perhaps a few other low-energy particles or resonances, notably the Δ , contribute most importantly from the right-hand side of (7). Since the difference between the energy denominators in the dispersion relations is negligible for integration over low-energy particles or resonances such as the N and Δ , it follows from the crossing symmetry between the A_+ and A_- amplitudes displayed in (7) that the amplitudes for $\gamma p \rightarrow \pi^+ n$ and $\gamma n \rightarrow \pi^- p$ must then be equal, as is indeed observed.

In the region of somewhat larger values of $-t$, $-0.2 \geq t \geq -0.8 \text{ GeV}^2$, the cross sections take on the characteristic ratios (1) and (2), and we know from recoil-proton polarization measurements that, at least for $\gamma p \rightarrow \pi^+ n$, the amplitudes have an imaginary part. There is no problem with the charge ratios for the imaginary part but we are left with the problem of the real part and there is no evidence that it is small, either from the polarization measurements, or from asymptotic energy-dependence considerations discussed in Sec. III. (If it were small then the smallness would have to be ex-

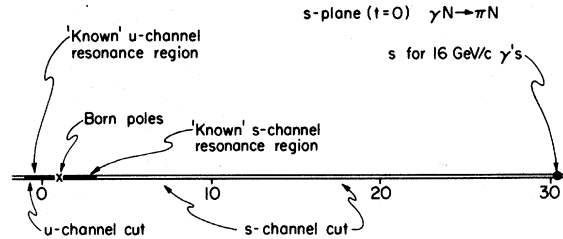


FIG. 4. The s -plane cut structure used in the fixed- t dispersion relations. The physical s value corresponding to incoming photon momentum of 16 GeV/c is shown, and the diagram illustrates that the dispersion-relation energy denominators $s' - s$ vary little as s' ranges over the low-energy cut region where the amplitudes are known. (The cut structure is shown for $t=0$; as $-t$ increases the left- and right-hand cuts move towards each other and eventually overlap.)

plained by a cancellation similar to that we are about to expound.) In this section, we examine the hypothesis that the combined contribution of the s - and u -channel *low*- and *medium*-energy imaginary parts (to the fixed- t dispersion relations giving the high-energy real part) is negligibly small. We use the term *low* and *medium* energy relative to the physical energy, and, for an s value of about 30 GeV^2 , the low- and medium-energy cuts might extend up to $s(u) \sim 5\text{--}15 \text{ GeV}^2$. If this be so it leaves the greater part of $\text{Re}A(s, t)$ free to come from the right-hand part of the s cut, say from $s' \gtrsim \frac{1}{2}s$, just from the smallness of the energy denominators on the right-hand part of the s -channel cut compared with the large ones from the left-hand part of the u -channel cut. Such a dominance of s -channel imaginary parts in the dispersion relation secures the charge ratios also in the real parts of the amplitudes.

To sustain our hypothesis we have to investigate whether integration over the low- and medium-energy regions is likely to give a negligibly small contribution to $\text{Re}A(s, t)$. The result is shown in Fig. 5, where we have plotted the contribution to $(s - M^2)^2 d\sigma/dt$ arising from the *real parts* only of the amplitudes, evaluated from the dispersion relations (7). The evaluation is done for an incident laboratory momentum of $16 \text{ GeV}/c$ [$s \approx 30 \text{ GeV}^2$], and the photoproduction helicity amplitudes used are those of Walker.⁹ We discuss the results in the region $-0.2 \geq t \geq -0.8 \text{ GeV}^2$.

The highest curve shown is that obtained by taking only the Born terms on the right-hand sides of

Eqs. (7a) and (7b) and in our t region the result is clearly impossible. If we add to the Born terms the effect of the $\Delta(1236)$ in both the s and u parts of the dispersion integral (7), we get a dramatic drop to the next highest curve, as shown. This effect was already noted by Engels, Schwiderski, and Schmidt¹⁰ in connection with photoproduction at energies between 1 and 3 GeV. Next, adding to the dispersion relations the $p_{11}(1470)$ and the $s_{11}(1560)$ again leads to a decrease, while there is a further dramatic drop on adding the $d_{13}(1520)$. We should note that at this stage the curve has already dropped to the level of the proton data for $-0.2 > t > -0.5 \text{ GeV}^2$, and to or below the level of the lowest neutron data for $-0.5 > t > -0.8 \text{ GeV}^2$. Adding the third resonance-region contribution to the dispersion relations leads to a further drop, but takes us to the end of the helicity-amplitude analysis of Walker. There is one more thing we can do in our examination of trends. The $f_{37}(1920)$ is a prominent Δ resonance, the first Regge recurrence of the $p_{33}(1236)$. If we assume that like the p_{33} , the $f_{37}(1920)$ has only magnetic coupling (as suggested for example by the quark model) and that the coupling is of the same sign as the p_{33} , and if we take the magnitude of the coupling from backward π^0 photoproduction,¹¹ then we get the bottom curve (over most of our t region) shown in Fig. 5. (In Walker's fit to the π^+ low-energy data nearly all the imaginary part is due to the resonances; the dots represent the final results when the nonresonant background at all energies is also taken into the dispersion integral.) The curves apply

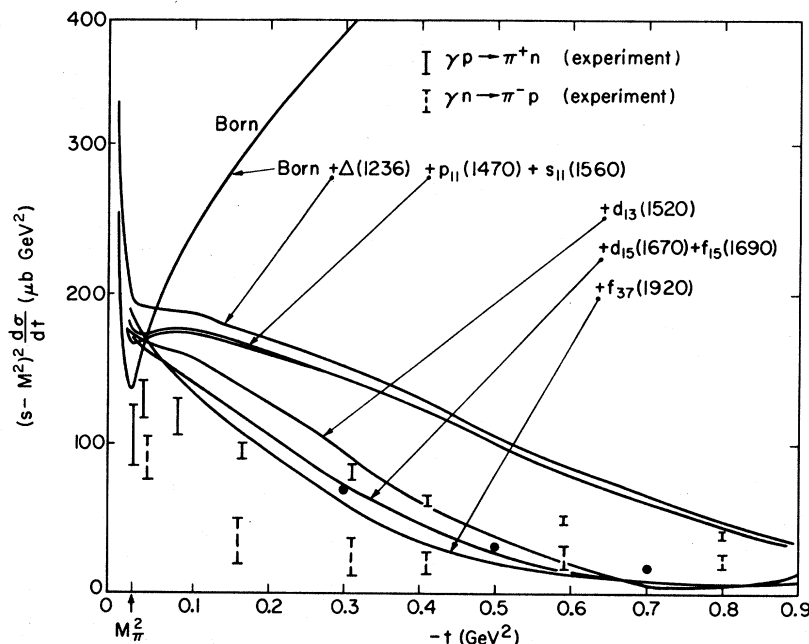


FIG. 5. The contribution to $(s - M^2)^2 d\sigma/dt$ arising from the real parts of the high-energy charged-pion photoproduction amplitudes as evaluated using the fixed- t dispersion relations (7). The various curves represent the results as singularities and resonances for successively higher s' are included in $\text{Im}A(s', t)$. The lowest curve is the result when all the resonances in the solid (Fig. 4) region are included plus the $f_{37}(1920)$ which is just outside the solid region. The dots show the result when the nonresonant background within the solid region is also included. The curves shown are for $\gamma p \rightarrow \pi^+ n$, but the $\gamma n \rightarrow \pi^- p$ curves are almost indistinguishable. The curves, and the experimental points showing the $\pi^+ n$ and $\pi^- p$ data, are also nearly independent of s , for s large.

with negligible error to either π^+ or π^- photoproduction, as is evident from the crossing symmetry in Eq. (7), since the variation of the energy denominators in the low-energy resonance region is small for large s .

The trend is obvious: As successively higher-mass resonances are added to both the s - and u -channel integrals in the fixed- t dispersion relations, the calculated real amplitudes get successively smaller, with the exception of the addition of $p_{11}(1470)$ which has a small influence in the opposite direction. In the interval $-0.5 > t > -0.8$ GeV² the result is already of the order of or smaller than the neutron data. The results are shown in another way in Fig. 6, where, at the fixed value of $t = -0.4$ GeV² we plot the same quantity as in Fig. 5 as a function of the upper limit of integration in the dispersion integrals. It is also obvious that the trend could continue since, though the partial-width higher-mass resonances are smaller, the residual amplitudes which they have to cancel are also smaller. We do not attach too much importance to the exact numbers obtained through the dispersion relations since, as pointed out by Walker⁹ and by others,¹² the results of the helicity-amplitude analysis in the present state of the data are subject to quite large errors.¹³⁻¹⁵ We rather point to the trend, which if continued will lead to the mutual cancellation of the low- and medium-energy resonances in the dispersion relations, and thus to satisfactory agreement

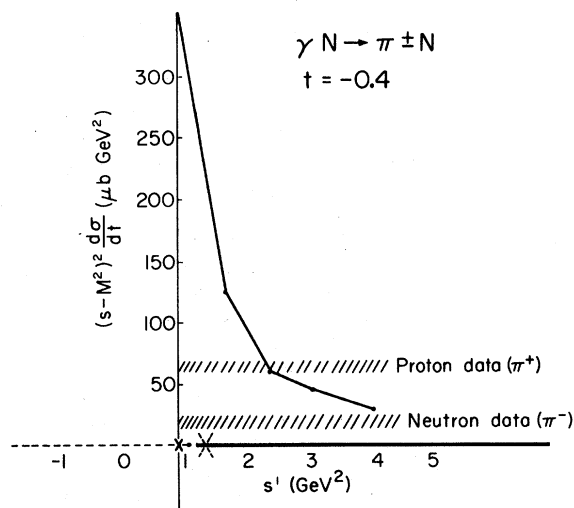


FIG. 6. The contribution to $(s - M^2)^2 d\sigma/dt$ of the real part of the high-energy amplitudes at a fixed value of $t = -0.4$ GeV², evaluated from the dispersion relations (7). The abscissa s' represents the cutoff in the upper limit of integration in (7), and the plotted line is the result of using (7) with upper limit of integration s' . (This graph can be obtained from the values given in Fig. 5 for $t = -0.4$ GeV².)

with the charge ratios for $\gamma p \rightarrow \pi^+ n$, $\gamma n \rightarrow \pi^- p$.

We may contrast this unidirectional effect of the resonances in the fixed- t dispersion relations in the region $-0.2 > t > -0.8$ GeV² to the varied effects in the extreme forward region. We plot the same quantities as before in Fig. 7, but now on the expanded horizontal scale of $(-t)^{1/2}$ appropriate to the extreme forward direction. The experimental points shown are $(s - M^2)^2 d\sigma/dt$ for $\gamma p \rightarrow \pi^+ n$, and the evidence is that the $\gamma n \rightarrow \pi^- p$ has an equal cross section for $(-t)^{1/2} < 0.2$ GeV². As before, the curves are the contributions to $(s - M^2)^2 d\sigma/dt$ of the real parts of the amplitudes calculated from the fixed- t dispersion relations (7) for various resonances included in the integrals. We see that the "Born + Δ " curve is significantly different from the "Born" curve but that the additional effect of adding all other "known" resonances is quite small, so that the final curve remains near "Born + Δ ." It is worth noting that one of the forward experimental points is considerably higher than "Born only" and agrees more nearly with "Born + Δ " and the other curves clustered around it. In view of the qualitative agreement of the experimental points and the curve, in the extreme forward direction all is compatible with (i) totally real amplitudes, (ii) saturation of the fixed- t dispersion relations by low-energy resonances, including the Born terms. Similar conclusions on the extreme forward region have been reached by previous authors.¹ Our only new

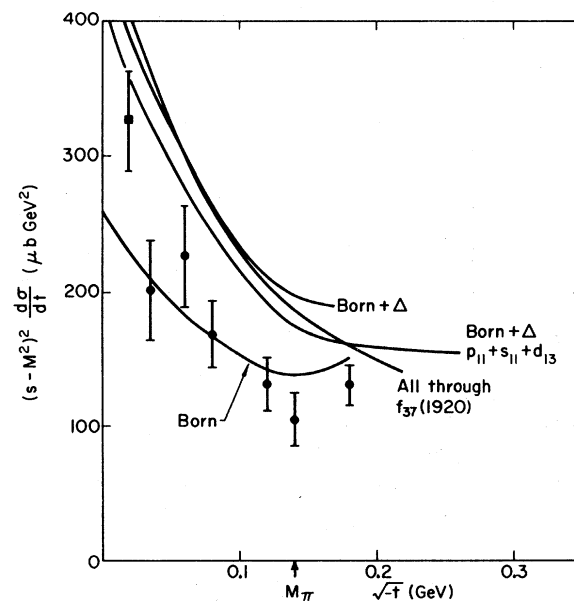


FIG. 7. The contribution to $(s - M^2)^2 d\sigma/dt$ of the real part of the high-energy amplitudes evaluated from the fixed- t dispersion relations, plotted as a function of $(-t)^{1/2}$ in the forward-spike region. The experimental points are for $\gamma p \rightarrow \pi^+ n$ at various energies (Ref. 2).

addition to their remarks is that the way the various resonances are contributing makes saturation seem likely, and that this *may* take place near the "Born + Δ " curve, at any rate for $(-t)^{1/2} \leq 0.05$ GeV.

In view of the importance of s -channel helicity in absorption models,⁶ or other models¹⁶ which view the nucleon as a spatially structured scattering object, it is interesting to set out the role of the various s -channel helicity amplitudes in the curves of Figs. 5, 6, and 7. To do this we introduce a mnemonic notation for the helicity amplitudes. For $\gamma N \rightarrow \pi N$ there are four independent helicity amplitudes and we take these to be the amplitudes for which the photon has helicity +1; in that case the initial helicity is $\frac{3}{2}$ or $\frac{1}{2}$ and the final one $\frac{1}{2}$ or $-\frac{1}{2}$. We name the helicity amplitudes corresponding to the various transitions as follows:

$$\begin{aligned} \frac{1}{2} \rightarrow \frac{1}{2} : H_0, \\ \frac{3}{2} \rightarrow \frac{1}{2} : H_1, \\ \frac{1}{2} \rightarrow -\frac{1}{2} : H_{-1}, \\ \frac{3}{2} \rightarrow -\frac{1}{2} : H_2, \end{aligned} \quad (8)$$

where the subscripts 0, ± 1 , and 2 represent no helicity flip, single helicity flip, and double helicity flip, respectively. We define the normalization and units of our helicity amplitudes to be the same as those of the helicity amplitudes H_1, H_2, H_3, H_4 of Walker's⁹ Eq. (21), so that

$$(H_0, H_1, H_{-1}, H_2) \equiv (H_2, H_1, H_4, H_3) \quad (9)$$

and

$$(s - M^2)^2 \frac{d\sigma}{dt} = 2\pi s (|H_0|^2 + |H_1|^2 + |H_{-1}|^2 + |H_2|^2). \quad (10)$$

We now describe the relative magnitudes of the various $\text{Re}H$ as evaluated from the dispersion relations (7). In the forward spike $\text{Re}H_0$ is strongly dominant, being at $t = -0.0002$ GeV² [$(-t)^{1/2} = 0.045$ GeV] more than ten times greater than any other amplitude. This of course is to be expected since the other (spin-flip) amplitudes must vanish at $\theta = 0$; in the language of Harari¹⁶ H_0 is a " J_0 " amplitude. Just outside the forward spike at $t = -0.02$ GeV² [$(-t)^{1/2} \sim m_\pi$], $\text{Re}H_0$ is still the largest amplitude, but only 40% larger than $\text{Re}H_2$; both $\text{Re}H_1$ and $\text{Re}H_{-1}$ are more than ten times smaller. At these two t values and in the spike region generally, there is only a few percent difference between $\text{Re}H_0$ evaluated using "Born + Δ " only, and evaluated using all the "known" amplitudes (the same holds for $\text{Re}H_2$).

The situation is very different in the region of principal interest, $-0.2 \geq t \geq -0.8$ GeV². Here, for "Born + Δ " only, $\text{Re}H_2$ is largest, $\text{Re}H_0$ is about 30% of $\text{Re}H_2$, and $\text{Re}H_1$ and $\text{Re}H_{-1}$ are very small. When

the full "known" amplitudes are taken in the dispersion relations, both $\text{Re}H_0$ and $\text{Re}H_2$ become considerably smaller (accounting for the drop in the curves of Fig. 5), while $\text{Re}H_1$ becomes non-negligible over a small range around $t = -0.3$ GeV² ($\text{Re}H_1$ is a " J_1 " amplitude and goes to zero at around $t = -0.75$ GeV²).

III. CONNECTION WITH FINITE-ENERGY SUM RULES

In the definition of the finite-energy sum rules (FESR) or continuous-moment sum rules (CMSR), it is implied that the connection between low and high energies is established through the assumption of some asymptotic or high-energy form, for which Regge poles are commonly used. Using the assumption that all the relevant Regge trajectories have small α , which, if correct, makes their result independent of any particular high-energy Regge model, Jackson and Quigg¹⁷ find a form for the real part of their high-energy amplitude in terms of an integral over the low-energy amplitude. The result is the same as if one were to evaluate the fixed- t dispersion relation (7), neglecting the variation with s' of the energy denominators; this is a good approximation for large energy s , and the comparatively small s' associated with the low-energy resonances. The FESR and CMSR evaluations are done for amplitudes having good $s \rightarrow u$ crossing properties; such amplitudes for photoproduction are the isoscalar-photon amplitude $A^{(0)}$ and the isovector-photon amplitudes $A^{(-)}$ and $A^{(+)}$ in terms of which the charged-pion photoproduction amplitudes of (7) are given by

$$\begin{aligned} A_{i+} &= \sqrt{2} (A_i^{(0)} + A_i^{(-)}), \\ A_{i-} &= \sqrt{2} (A_i^{(0)} - A_i^{(-)}), \quad i = 1, 2, 3, 4. \end{aligned} \quad (11)$$

$A_i^{(0)}, A_i^{(+)}, A_j^{(-)}$ are crossing even and $A_j^{(0)}, A_j^{(+)}, A_i^{(-)}$ are crossing odd for $i = 1, 2, 4$ and $j = 3$. The calculations of Jackson and Quigg are for isovector ($-$) amplitudes (they use t -channel helicity amplitudes), so they are approximately proportional to the *difference* of the $\gamma p \rightarrow \pi^+ n$ amplitudes (A_{i+}) and $\gamma n \rightarrow \pi^- p$ amplitudes (A_{i-}) calculated by our method of fixed- t dispersion relations.

From the crossing relations, as exhibited in Eq. (7a), the high-energy amplitudes $\text{Re}A_{i+}$ and $\text{Re}A_{i-}$ calculated by fixed- t dispersion relations using the low-energy amplitudes are approximately equal and of opposite sign for $i = 1, 2, 4$; $A_{3\pm}$ are of the same sign but turn out to be smaller. Consequently, from (7), our calculated $\text{Re}A$ are dominated by the isovector amplitudes $\text{Re}A^{(-)}$. We agree with Jackson and Quigg that the cross section of the forward spike is dominated by $\text{Re}A^{(-)}$ as calculated from low-energy amplitudes, and we have reinforced

that conclusion by observing the convergent behavior of the amplitudes in that t region as a function of integration cutoff. But Jackson and Quigg also find agreement with some "average" of the $\gamma p \rightarrow \pi^+ n$ and $\gamma n \rightarrow \pi^- p$ cross sections over a much larger range of t . We would not attach any significance at all to this pseudomodel for $|t| \geq 0.2 \text{ GeV}^2$ and we rather consider the rough agreement attained to be a fortuitous consequence of the particular integration cutoff which follows from our present state of knowledge of the low-energy amplitudes; to support this we pointed out in Sec. II the behavior of the calculated real amplitudes as a function of integration cutoff in the region $-0.2 \geq t \geq -0.8 \text{ GeV}^2$, which is qualitatively different from that in the spike region.

We point out one quite general feature associated with the decomposition (11) into isoscalar and isovector amplitudes of good crossing properties. At high energies, $d\sigma/dt$ is proportional to $1/s^2$, while the polarized-target experiments¹⁸ reveal that there are both a real and an imaginary part in important amplitudes. The simplest possibility to account for both these facts is that both the real and the imaginary part of the invariant amplitudes are proportional to $1/s$. If then the amplitudes are in a non-oscillatory asymptotic region and contain no logarithmic terms one can, as usual, apply the Phragmen-Lindeloff theorem to show that crossing-even amplitudes are pure imaginary and crossing-odd amplitudes are pure real. From Eq. (11) and the crossing properties of the $A_i^{(0)}$ and $A_i^{(-)}$ it would then follow that

$$\frac{d\sigma}{dt}(\gamma p \rightarrow \pi^+ n) = \frac{d\sigma}{dt}(\gamma n \rightarrow \pi^- p),$$

which is contrary to experiment. The conclusion is that we do not have a simple asymptotic regime of the type just outlined and in support we note that the polarization at 5 GeV/c is different from that at 16 GeV/c. It would be interesting to have results over a considerable range of high energies in various types of polarization experiments to elucidate the situation.

IV. CHARGED-PION PHOTOPRODUCTION BY POLARIZED PHOTONS

If σ_{\perp} and σ_{\parallel} are the cross sections for $\gamma N \rightarrow \pi N$ with photons polarized perpendicular and parallel to the production plane, respectively, then at high energies σ_{\perp} comes wholly from natural-parity t -channel exchange and σ_{\parallel} from unnatural-parity t -channel exchange. At 3 GeV/c the asymmetry ratio $A^{\pm} = (\sigma_{\perp} - \sigma_{\parallel})/(\sigma_{\perp} + \sigma_{\parallel})$ has been measured for π^{\pm} photoproduction, respectively. It is found that the asymmetry ratio A^+ for $\gamma p \rightarrow \pi^+ n$ is $A^+ \approx 0.7$ in the range $-0.2 > t > -0.8 \text{ GeV}^2$ while the ratio A^- for $\gamma n \rightarrow \pi^- p$ is $A^- \approx 0.0$ in the same t range. Within the

suggested quark model, $A^+ = A^-$ (since the only difference in the model is in the charge of the proton quark and that of the neutron quark) giving an apparent disagreement between the data and the model. However, the cross section for π^- production is small, so we would expect a large proportion of this amplitude to be outside the model, for example from pion exchange which is of unnatural parity and contributes to σ_{\parallel} , thus reducing A . Indeed for $-0.2 > t > -0.8 \text{ GeV}^2$ the charge ratio $\sigma_{\perp}(\gamma n \rightarrow \pi^- p)/\sigma_{\perp}(\gamma p \rightarrow \pi^+ n)$ is close to the exact model value of 25%, while the charge ratio for σ_{\parallel} is approximately unity. The inference is that the model contributes only to σ_{\perp} (natural-parity exchange) which dominates $\gamma p \rightarrow \pi^+ n$ and that the smaller σ_{\parallel} (unnatural-parity exchange) only becomes important for $\gamma n \rightarrow \pi^- p$.

We show in Fig. 8 the ratio $A = (\sigma_{\perp} - \sigma_{\parallel})/(\sigma_{\perp} + \sigma_{\parallel})$ of the high-energy real parts as evaluated by the fixed- t dispersion relations from the low-energy resonances.

V. π^0 PHOTOPRODUCTION

In Fig. 9 we plot the contribution to the high-en-

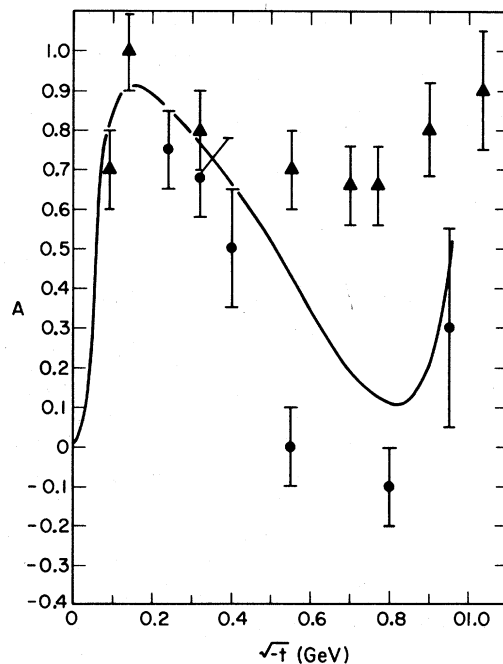


FIG. 8. The curve shows the high-energy $\gamma p \rightarrow \pi^+ n$ or $\gamma n \rightarrow \pi^- p$ asymmetry ratio $A = (\sigma_{\perp} - \sigma_{\parallel})/(\sigma_{\perp} + \sigma_{\parallel})$ for polarized photons, where σ_{\perp} and σ_{\parallel} are the contributions to the cross sections from the real parts evaluated using the fixed- t dispersion relations, integrated over the low-energy resonances. Some representative experimental points³ are shown as \blacktriangle for $\gamma p \rightarrow \pi^+ n$ and \bullet for $\gamma n \rightarrow \pi^- p$.

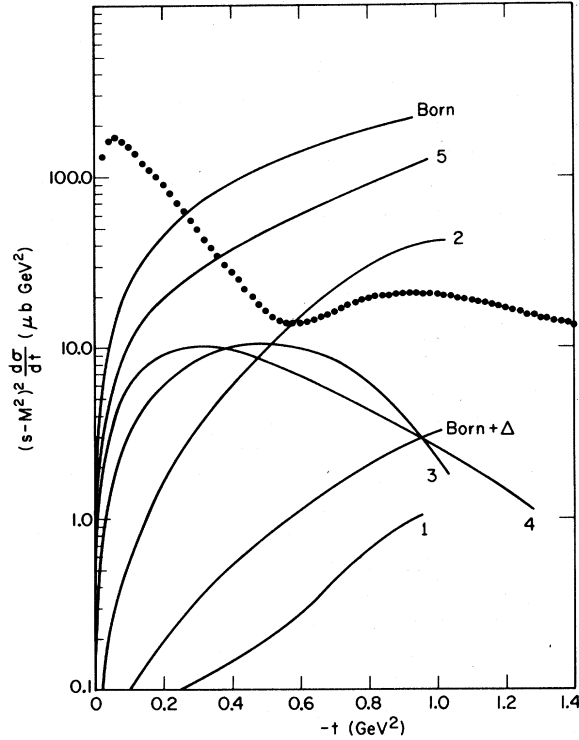


FIG. 9. The contribution to $(s - M^2)^2 d\sigma/dt$ arising from the real parts of the high-energy $\gamma p \rightarrow \pi^0 p$ photoproduction amplitudes as evaluated using the fixed- t dispersion relations (7) at 16 GeV/c. The different curves show the inclusion of successively higher-mass resonances in (7) and the solid circles are a representation of the experimental high-energy data. Curves 1, 2, 3, and 4 include resonances through, respectively, $s_{11}(1560)$, $d_{13}(1520)$, $f_{15}(1690)$, $f_{37}(1920)$. Curve 5 includes resonances plus nonresonant background.

ergy π^0 photoproduction cross section of the real parts of the amplitudes evaluated by the fixed- t dispersion relations. We show curves corresponding to the inclusion of successively higher-mass resonances in the dispersion relations, as in the charged-pion case. Unlike the charged-pion case there is no uniform tendency; but like the charged-pion case (for $-0.2 \geq t \geq -0.8$ GeV 2) there is no evidence of saturation of the dispersion relations by the low-energy resonances. When we bear in mind the uncertainties of the present data and the resulting partial-wave analyses, it is probably not worthwhile to comment further on the confusing situation evident in Fig. 9.

There is no simple prediction on the ratio of neutral to charged-pion photoproduction. However, if one considers the ratio

$$R_0 = \frac{d\sigma}{dt}(\gamma p \rightarrow \pi^0 p) \bigg/ \frac{d\sigma}{dt}(\gamma n \rightarrow \pi^0 n), \quad (12)$$

it was shown in Ref. 19 by arguments based on our simple quark model of Fig. 2(a) that

$$\frac{4}{49} \leq R_0 \leq \frac{16}{25}. \quad (13)$$

It should be emphasized that the arguments leading to (13) involve the quark spins and thus (13) has not quite the same status as the charge ratios (5) and (6). The experiments give results at or somewhat above the upper limit in (13), leading, as shown in Ref. 19, to quark-spin scalar dominance and strong dominance of σ_{\perp} in neutral-pion photoproduction. Recent experimental results on the asymmetry $A = (\sigma_{\perp} - \sigma_{\parallel})/(\sigma_{\perp} + \sigma_{\parallel})$ in π^0 photoproduction show that A is in the region of 0.9 to 1.0, corresponding to strong dominance of σ_{\perp} , except in the region of $t = -0.6$ GeV 2 where there is a drop in A to about $A = 0.8$. At $t = -0.6$ GeV 2 there is the well-known dip in π^0 photoproduction, where presumably processes from outwith the model become relatively more important.

VI. DISCUSSION AND CONCLUSIONS

We have noted in Sec. I how the duality diagrams, combined with some weak vector-meson-dominance assumptions, lead to certain ratios for the imaginary parts of the amplitudes, $\text{Im} A$, for $\gamma N \rightarrow \pi^{\pm} N$ and $\gamma N \rightarrow \pi^{\pm} \Delta$; we have shown how the same ratios follow in an explicit quark model. Experimentally, and in the region $-0.2 \geq t \geq -0.8$ GeV 2 , the predicted ratios on $|\text{Im} A|^2$ hold for $d\sigma/dt$ which is proportional to $|\text{Im} A|^2 + |\text{Re} A|^2$; since the ratios are not predicted for $\text{Re} A$, because of the contribution to $\text{Re} A$ of distant u -channel resonances, a problem is posed. The suggested resolution of the problem is that the combined contributions to $\text{Re} A$ of the "low- and medium-energy" s - and u -channel resonances are negligible, so that $\text{Re} A$ is either small compared to $\text{Im} A$ or dominated by the "high-energy" s -channel resonances which would maintain the charge ratios in $\text{Re} A$. By explicit calculation, using fixed- t dispersion relations for $\gamma N \rightarrow \pi^{\pm} N$, it was shown that the cancellation of the contributions of low-energy s - and u -channel resonances to $\text{Re} A$, is strongly suggested by our present knowledge of the low-energy resonances (and the associated $\text{Im} A$) from multipole analysis. On the other hand, in the region $0 > t > -0.2$ GeV 2 , where the cross sections for $\gamma p \rightarrow \pi^+ n$ and $\gamma n \rightarrow \pi^- p$ are tending towards equality in the forward direction, the fixed- t dispersion relations are dominated by the very-low-energy s - and u -channel resonances, in particular by the (gauge-invariant) Born terms and the Δ ; thus $(d\sigma/dt)_{\text{exp}} \approx (\text{Re} A)^2$, where $\text{Re} A$ is found from the fixed- t dispersion relations.

The charge ratios for the imaginary part of the $\gamma N \rightarrow \pi^{\pm} N$ photoproduction amplitudes are given by

$$\text{Im} A(\gamma n \rightarrow \pi^- p) / \text{Im} A(\gamma p \rightarrow \pi^+ n) = \frac{1}{2}. \quad (14)$$

The duality-diagram relations which, together with the assumption that a photon couples to vector mesons as a U -spin scalar, lead to (14) are⁷

$$\text{Im}(\pi^- p \rightarrow \omega^0 n) = -\text{Im}(\pi^- p \rightarrow \rho^0 n), \quad (15a)$$

$$\text{Im}(\pi^+ n \rightarrow \omega^0 p) = -\text{Im}(\pi^+ n \rightarrow \rho^0 p). \quad (15b)$$

Since the square of (14) holds experimentally for the cross sections, ($\propto |\text{Im} A|^2 + |\text{Re} A|^2$) in the region $-0.2 > t > -0.8 \text{ GeV}^2$, it is interesting to see whether the squares of (15) also hold experimentally for the cross sections ($\propto |\text{Im} A|^2 + |\text{Re} A|^2$) in the same t region. We do have experimental information²⁰ both on $\pi^+ n \rightarrow \omega^0 p$ and $\pi^+ n \rightarrow \rho^0 p$ which suggests that, for $-0.2 > t > -0.8 \text{ GeV}^2$,

$$\frac{d\sigma}{dt}(\pi^+ n \rightarrow \omega^0 p) \simeq \frac{d\sigma}{dt}(\pi^+ n \rightarrow \rho^0 p). \quad (16)$$

Another duality-diagram prediction, related to $\gamma N \rightarrow \pi \Delta$, for which information exists on the corresponding cross section is

$$\text{Im}(\pi^+ p \rightarrow \omega^0 \Delta^{++}) = \text{Im}(\pi^+ p \rightarrow \rho^0 \Delta^{++}) \quad (17)$$

and experimentally,²¹ for $-0.2 > t > -0.8 \text{ GeV}^2$,

$$\frac{d\sigma}{dt}(\pi^+ p \rightarrow \omega^0 \Delta^{++}) / \frac{d\sigma}{dt}(\pi^+ p \rightarrow \rho^0 \Delta^{++}) \simeq 1.5, \quad (18)$$

which is perhaps in slightly worse agreement with the square of (17) than the photoproduction cross sections (2) are with (6). (We wish to remark on the empirical status of our observations that the duality-diagram relations hold good for the whole amplitude, in certain cases, and that concomitantly in π^\pm photoproduction the contributions of the low-energy s - and u -channel resonances to the high-energy amplitude cancel. Since we have no theory we cannot foretell that such relations hold for all reactions. In particular similar whole-amplitude duality-diagram relations may very well *not* hold for kaon-initiated reactions, since here the s and u channels have a dissimilar nature, one being exotic and one nonexotic.)

In the extreme forward direction $0 > t > -0.1 \text{ GeV}^2$, for²⁰ $\pi^+ n \rightarrow \rho^0 p$, $\omega^0 p$ and for²² $\pi^- p \rightarrow \rho^0 n$ the ρ^0 cross section rises as $-t$ tends to zero and the ω^0 cross section falls to zero, agreeing with the photoproduction through a vector-meson-dominance prescription.²³ Another way of stating this comparison, independently of any vector-meson-dominance

assumption, is that the experiments on both $\gamma N \rightarrow \pi^\pm N$ and $\pi^\pm N \rightarrow \rho^0 N$, $\pi^\pm N \rightarrow \omega^0 N$ in the extreme forward direction ($0 > t > -0.1 \text{ GeV}^2$) are in some rough agreement with the Born approximation. It would be interesting to investigate in more detail the contribution of the Born approximation and other low-energy resonances (such as the lowest decuplet) to the real parts of the amplitudes for other nonelastic high-energy two-body reactions in the extreme forward direction.

If we were to take the naive quark model seriously, we might have in mind the following picture of forward pion photoproduction. In the region of very small invariant four-momentum transfer, the (gauge-invariant) Born-approximation amplitudes for $\gamma N \rightarrow \pi^\pm N$ represented by the diagrams of Fig. 3(a) for $\gamma N \rightarrow \pi^\pm N$ are important, maybe dominant, and give a forward spike. The amplitudes with Δ as intermediate state illustrated in Fig. 3(b) when added to the Born terms give a more pronounced forward spike, as shown in Fig. 7. This is compatible with a composite model insofar as for small momentum transfer the quark that is struck by the photon will tend to remain in the same spatial state, so that the intermediate state will tend to be that of the nucleon itself or the Δ which has the same spatial wave function as the nucleon in the quark model, as in the nucleon pole term of the Born approximation. When the struck quark is not excited the sum over intermediate states allows the pion to be emitted from a quark other than that which interacts with the photon [Fig. 3(c)]; when such emissions from all possible quarks are taken into account we then regain the nucleon pole as an important part of the composite model. Strongly varying extreme forward behavior, also presumably associated with a gauge-invariant pion-pole term, is observed for $\gamma N \rightarrow \pi^\pm \Delta$. At larger $-t$ than the extreme forward, or pion-pole region, spatial excitation of the quarks becomes more important and the photoproduction situation is as in Fig. 2(a), leading to the charge ratios discussed above in the region $-0.2 \geq t \geq -0.8 \text{ GeV}^2$. For $-0.8 \text{ GeV}^2 > t$ one is in another region, which would presumably correspond, in the quark model, to stronger interactions of the initially excited quark with the other quarks—that is, to multiple scattering.

The authors would like to thank Dr. David Lyth for a helpful conversation.

*This work was supported in part by the U. S. Atomic Energy Commission.

†Permanent address: Glasgow University, Glasgow, Scotland.

¹B. Richter, in *Proceedings of the Third International Symposium on Electron and Photon Interactions at High Energies, Stanford Linear Accelerator Center, Stanford, California, 1967* (Clearing House of Federal

- Scientific and Technical Information, Washington, D. C., 1968), p. 309; H. Harari, *ibid.*, p. 337; N. Dombey, Phys. Letters 30B, 646 (1969).
- ²A. M. Boyarski, F. Bulos, W. Busza, R. Diebold, S. D. Ecklund, G. E. Fischer, J. R. Rees, and B. Richter, Phys. Rev. Letters 20, 300 (1968).
- ³C. Geweniger, P. Heide, U. Kötz, R. A. Lewis, P. Schmüser, H. J. Skronn, H. Wahl, and K. Wegener, Phys. Letters 29B, 41 (1969); K. Lubelsmeyer, in *International Symposium on Electron and Photon Interactions at High Energies, Liverpool, England, 1969*, edited by D. W. Braben and R. E. Rand (Daresbury Nuclear Physics Laboratory, Daresbury, Lancashire, England, 1970), p. 45.
- ⁴B. Richter, in *Proceedings of the Fourteenth International Conference on High-Energy Physics, Vienna, 1968*, edited by J. Prentki and J. Steinberger (CERN, Geneva, 1968); K. Lubelsmeyer, Ref. 3, p. 45.
- ⁵J. A. Campbell, R. B. Clark, and D. Horn, Phys. Rev. D 2, 217 (1970).
- ⁶G. L. Kane, F. Henyey, D. R. Richards, M. Ross, and G. Williamson, Phys. Rev. Letters 25, 1519 (1970).
- ⁷The possibility of relations arising thus between the imaginary parts of photoproduction amplitudes was envisaged by H. Harari, Phys. Rev. Letters 22, 562 (1969).
- ⁸See, for example, F. A. Berends, A. Donnachie, and D. L. Weaver, Nucl. Phys. B4, 3 (1967).
- ⁹R. L. Walker, Phys. Rev. 182, 1729 (1969).
- ¹⁰J. Engels, G. Schwiderski, and W. Schmidt, Phys. Rev. 166, 1343 (1968).
- ¹¹G. Buschhorn, P. Heide, U. Kötz, R. A. Lewis, P. Schmüser, and H. J. Skronn, Phys. Rev. Letters 20, 230 (1968).
- ¹²R. G. Moorhouse and W. A. Rankin, Nucl. Phys. B23, 181 (1970).
- ¹³In particular: (i) The large uncertainty for the $p_{11}(1470)$ pointed out in Ref. (12); (ii) As pointed out in Refs. (15) and (14) it is now believed that f_{15} photo-production from neutrons is small, in contradiction with the Walker analysis.
- ¹⁴R. L. Walker, in *International Symposium on Electron and Photon Interactions at High Energies, Liverpool, England, 1969*, edited by D. W. Braben and R. E. Rand, Ref. 3.
- ¹⁵L. A. Copley, G. Karl, and E. Obryk, Nucl. Phys. B13, 303 (1969).
- ¹⁶H. Harari, Ann. Phys. (N.Y.) (to be published).
- ¹⁷J. D. Jackson and C. Quigg, Phys. Letters 39B, 236 (1969); Nucl. Phys. B22, 301 (1970).
- ¹⁸C. C. Morehouse *et al.*, Phys. Rev. Letters 25, 835 (1970).
- ¹⁹I. Barbour and R. G. Moorhouse, Nucl. Phys. B20, 629 (1970).
- ²⁰G. Bellettini, in *Proceedings of the Fourteenth International Conference on High-Energy Physics, Vienna, 1968*, edited by J. Prentki and J. Steinberger, Ref. 4; P. B. Johnson *et al.*, Phys. Rev. 176, 1051 (1968).
- ²¹G. S. Abrams *et al.*, Phys. Rev. Letters 25, 617 (1970).
- ²²F. Bulos *et al.*, SLAC report (unpublished).
- ²³C. F. Cho and J. J. Sakurai, Phys. Rev. D 2, 517 (1970).